J Mater Sci: Mater Electron (2016) 27:7192–7199
DOI 10.1007/s10854-016-4683-2

Synthesis, characterization and photocatalytic property of nickel sulfide nanoparticles

Yousef Fazli[1] · Seied Mahdi Pourmortazavi[2] · Iraj Kohsari[3] · Meisam Sadeghpour Karimi[4] · Majid Tajdari[5]

Received: 7 January 2016 / Accepted: 12 March 2016 / Published online: 19 March 2016

Abstract Nickel sulfide nanoparticles were prepared by a facile chemical procedure with a low cost, low temperature method without any template. The chemical precipitation reaction was optimized by Taguchi robust route and analysis of variance to obtain nickel sulfide nanoparticles with smallest size and uniform morphology. Analysis of variance (ANOVA) was utilized for quantitative evaluation of the parameters contributions on the size of formed NiS particles. The ANOVA showed that 0.1 mol/L as concentration of nickel reagent, 0.005 mol/L concentration of sulfide ion, and 40 °C as the temperature of the reactor are optimal conditions for production of NiS nanoparticles. The resulted nanoparticles at optimum conditions have an average size about 20 ± 3 nm. The morphology, microstructure, composition, thermal and optic behaviors of as-synthesized nickel sulfide nanoparticles were evaluated by various techniques, i.e., field emission-scanning electron microscopy, transmission electron microscopy, X-ray diffraction, Fourier transform-infrared spectroscopy, and ultraviolet–visible diffuse reflectance spectroscopy. The prepared nickel sulfide nanoparticles were also used as a photocatalyst in water treatment and the results show their potential in the elimination of organic pollution.

✉ Seied Mahdi Pourmortazavi
pourmortazavi@yahoo.com

[1] Department of Chemistry, Faculty of Science, Arak Branch, Islamic Azad University, Arak, Iran

[2] Faculty of Material and Manufacturing Technologies, Malek Ashtar University of Technology, P.O. Box 16765-3454, Tehran, Iran

[3] Department of Chemistry, Amir-Kabir University of Technology, Tehran, Iran

[4] Faculty of Chemistry and Chemical Engineering, Malek Ashtar University of Technology, Tehran, Iran

[5] Department of Chemical Engineering, Faculty of Engineering, Arak Branch, Islamic Azad University, Arak, Iran

1 Introduction

Recently investigations on synthesis and characterization of inorganic nanomaterials with specific morphology have received considerable attention, while their applications have become an active field in science and technology. This trend is due to the high utility of nanomaterials for designing new products with the novel or specific properties in order to application in different fields, i.e., catalysts, photocatalyst, photonics, nanoscale electronics, ceramics, pigments and dye industries [1–5]. Nanostructured materials (i.e., nanowires, nanotubes, nanobelts, and nanorods) have obtained considerable attention from the scientific community due to their novel physicochemical properties and potential applications of nanomaterials in various areas of science and technology [6–9]. The efforts directed toward understanding the magnetic, electronic, and optical properties of these nanostructures have been developed because of the unique properties of the nanomaterials in comparison with their bulk counterparts [10–12].

Metal sulfides exhibit interested electronic properties which these characteristics lead to achieving some technological applications for this family of materials [13, 14]. Nickel sulfide as a member of this family has been obtained much attention due to its potentials for application as a transformation toughening agent for the used materials in different semiconductors, catalysts, and cathodes of rechargeable lithium batteries [14, 15]. Furthermore, binary Ni–S systems such as $Ni_{3+x}S_2$, Ni_3S_2, Ni_4S_{3+x}, Ni_6S_5,

Ni_7S_6, Ni_9S_8, NiS, Ni_3S_4, and NiS_2 are highly interested because of possessing multi-phases [16]. Nickel sulfide may be formed as two crystal structures (α and β) depending on the temperature. The alpha form posesses a hexagonal phase ($P6_3/mmc$) which forms at high temperatures, while the beta form has a rhombohedral cell unit (R3m) that is formed at low temperatures [17, 18].

Up to date different shapes of nickel sulfide nanoparticles i.e., nanospheres, nanorods, nanoprisms, nanoneedles, hollowspheres, flower-like architectures, urchin-like nanocrystallines, layer-rolled structures, etc. have been synthesized by various methods [19]. These forms of nickel sulfide nanostructures could be obtained by hydrothermal [20, 21], solvothermal [22–24], molecular procedure [25], and precipitation routes [26]. However, the influence of nanoparticles morphlogies on their physicochemical behavior caused interesting of any further effort for tunable synthesis of uniform nickle sulfide nanoparticles.

Optimization is a critical step in developing of a nanomaterials synthesis procedure. Fractional factorial experiment designs decrease significantly the number of required trials for optimization of the investigated process parameters [27–29]. The other advantage of fractional factorial rather than sequential design is the possibility for extraction of more information from the resulted experimental data. The principals, theory, and methodology of Taguchi experiment design as a statistical optimization method for the evaluation of chemical procedures have been explained in detail elsewhere [30–37]. In this study, an orthogonal array was used to optimize the chemical precipitation of nickel sulfide nanoparticles by investigation on several experimental variables, i.e., nickel and sulfide reagent concentrations, nickel reagent feeding flow rate and temperature of reactor on the size of related nickel sulfide particles. To the best our knowledge, synthesis of submicron and nano-structures of nickel sulfide by several techniques [19–26] previously has been reported in the literature. But, there is no report on statistical optimization of the nickel sulfide nanospheres synthesis by chemical precipitation method without use of a catalyst, surfactant or template.

2 Experimental

2.1 Material and procedure

Analytical-grade nickel nitrate and sodium sulfide as reagents were used as received from the Merck Company (Germany). Nickel sulfide particles were prepared by chemical precipitation reaction in aqueous media by feeding of Ni^{2+} solution directly to the sulfide solution in the reactor under ultrasound irradiation and vigorous stirring in the definite temperature. After finishing the precipitation reaction, the formed nickel sulfide powder was centrifuged and then washed with distilled water three times. After completing the chemical precipitation process, the formed NiS particles were introduced to an autoclave and treated under hydrothermal conditions (190 °C temperature for 24 h). Thereafter, the resulted precipitate was washed with absolute ethanol and dried at 80 °C during 4 h. The experimental parameters of the precipitation reaction were optimized by the aid of an experimental design approach (Taguchi robust design) to the synthesis nickel sulfide nanoparticles. The investigated variables were included Ni^{2+} concentration, S^{2-} concentration, feeding flow rate of nickel reagent to the sulfide solution and temperature of reactor as shown in Table 1.

2.2 Characterization of synthesized nickel sulfide particles

The synthesized nickel sulfide samples were characterized by field emission scanning electron microscope (FE-SEM). The FE-SEM images were recorded on a Hitachi S-4160 series instrument. Transmission electron microscope (TEM) images were recorded on a Ziess-EM10C scanning electron microscope. The sample preparation was carried out via coating on carbon coated grid Cu Mesh 300 prior to the measurement. X-ray powder diffraction (XRD) analysis was carried out on a Rigaku D/max 2500 V diffractometer equipped with the graphite monochromator and Cu target. Fourier transform infrared (FTIR) spectra of nickel sulfide nanoparticles were recorded on a Perkin-Elmer (spectrum two) spectrophotometer in the wavenumber range of 4000–500 cm^{-1} by the use of KBr pellet technique. The UV–Vis diffuse reflectance spectra were recorded at room temperature using Avantes Spectrometer Avaspec-2048-TEC. The UV–Vis spectra of the water pollution treatment were recorded by Perkin-Elmer Lmbda 25 UV/Vis spectrometer.

2.3 Photocatalytic activities

In this study, a quartz double pipe photocatalytic reactor was used, while UV irradiation was supplied by a UV lamp (250 W) inserted inside of the interior pipe of the reactor. In each experiment, 200 mL aqueous solution of 50 mg/L methylene blue (MB) was added to the reactor. Then, 40 mg of as-prepared nanoparticles was dispersed in this solution. Sampling during the illumination was carried out every 20 min. The UV–Vis absorption spectra of the resulted samples were obtained.

Table 1 Applied OA_9 (3^4) matrix for parameter optimization in synthesis of nanoparticles by chemical precipitation

Run number	Ni^{2+} concentration (M)	S^{2-} concentration (M)	Ni^{2+} feed flow rate (mL/min)	Temperature (°C)	Average size of nickel sulfide particles (nm)
1	0.005	0.005	2.5	20	37
2	0.005	0.01	10.0	40	32
3	0.005	0.1	40.0	60	35
4	0.01	0.005	10.0	60	26
5	0.01	0.01	40.0	20	39
6	0.01	0.1	2.5	40	26
7	0.1	0.005	40.0	40	20
8	0.1	0.01	2.5	60	32
9	0.1	0.1	10.0	20	33

3 Results and discussion

3.1 Nickel sulfide synthesis procedure and optimization strategy

Introducing a cation with an anion in order to their reaction under ultrasound irradiation and formation of their water insoluble inorganic salt i.e., nickel sulfide could be considered as a facile synthesis method for insoluble materials. However, tuning the morphology of product in such precipitation reactions is complex. Fortunately, revelation and tuning the individual effects of different process parameters on product particle size with the aid of statistical optimization methods could be as a shortcut [38]. Therefore, the effects of several variables, i.e., concentrations of Ni^{2+} and S^{2-} in aqueous reagents, the flow rate for Ni^{2+} reagent feeding to S^{2-}, and temperature of the reactor during the sonicated precipitation process on the size of nickel sulfide particles were investigated at triple levels as reported in Table 1. FESEM images presented in Fig. 1 correspond to some of the nickel sulfide samples produced in different experimental conditions of Table 1. The images confirm that the size of nickel sulfide particles obtained at various experimental conditions is dissimilar. In other word, the size of nickel sulfide particles is dependent on the operating conditions. Meanwhile, in the last column of Table 1 the average size of synthesized nickel sulfide particles at each run is presented. By the use of these data as input, the average size of nickel sulfide particles correspond to the effect of each studied factor at any level was computed [29, 39] and the obtained results are presented in Fig. 2 as bar graphs. These graphs show the trend in variation of nickel sulfide particle size as a function of studied factor's level. Figure 2a, b show the effects of Ni^{2+} and S^{2-} concentrations as the reagents on the size of precipitated nickel sulfide particles at triple levels (0.005, 0.01, and 0.1 mol/L), respectively. As seen, 0.1 M as the concentrations of nickel reagent and 0.005 M as the concentration of sulfide reagent are the optimum concentrations for precipitation of nickel sulfide particles with the smallest size. The effect of nickel reagent feeding flow rate (2.5, 10, and 40 mL/min) on the size of nickel sulfide particles was also studied (Fig. 2c). It was found that variation of the nickel reagent flow rate leads to the mild change in the size of precipitated nickel sulfide particles. Meantime, 40 °C is the optimum temperature for precipitation of nickel sulfide nanoparticles among the triple studied levels (20, 40 and 60 °C) for this variable (Fig. 2d).

The analysis of variance (ANOVA) was carried out on the resulted data to evaluate the significance of studied variables in tuning the size of nickel sulfide particles and the outcomes are shown in Table 2. ANOVA data (at 90 % confidence interval) revealed that, except nickel reagent feeding flow rate, all other studied variables (i.e., nickel ion concentration, sulfide ion concentration, and temperature) have significant roles in defining the size of formed nickel sulfide particles, whereas the probable interactions between the studied variables were ignored. Meanwhile, these results proposed that the optimum conditions for preparation of nickel sulfide particles with less size via studied precipitation reaction are as follow: 0.1 mol/L concentration of nickel ion reagent, 0.005 mol/L concentration of sulfide ion reagent, and 40 °C as the reactor temperature. As proposed in Taguchi experiment design [40, 41], the size of nickel sulfide particles at optimum conditions of the proposed process is predictable via the following expression:

$$Y_{opt} = \frac{T}{N} + \left(C_{Ni} - \frac{T}{N}\right) + \left(C_s - \frac{T}{N}\right) + \left(t_r - \frac{T}{N}\right)$$

In this equation, T/N represents the average size of nickel sulfide particles obtained during designed experiments; while, T is the summation of all results, N is the total number of performed experiments, Y_{opt} is the nickel sulfide particle size at optimum conditions, C_{Ni}, C_S, and t_r are the average size of product (Fig. 2) at the optimum

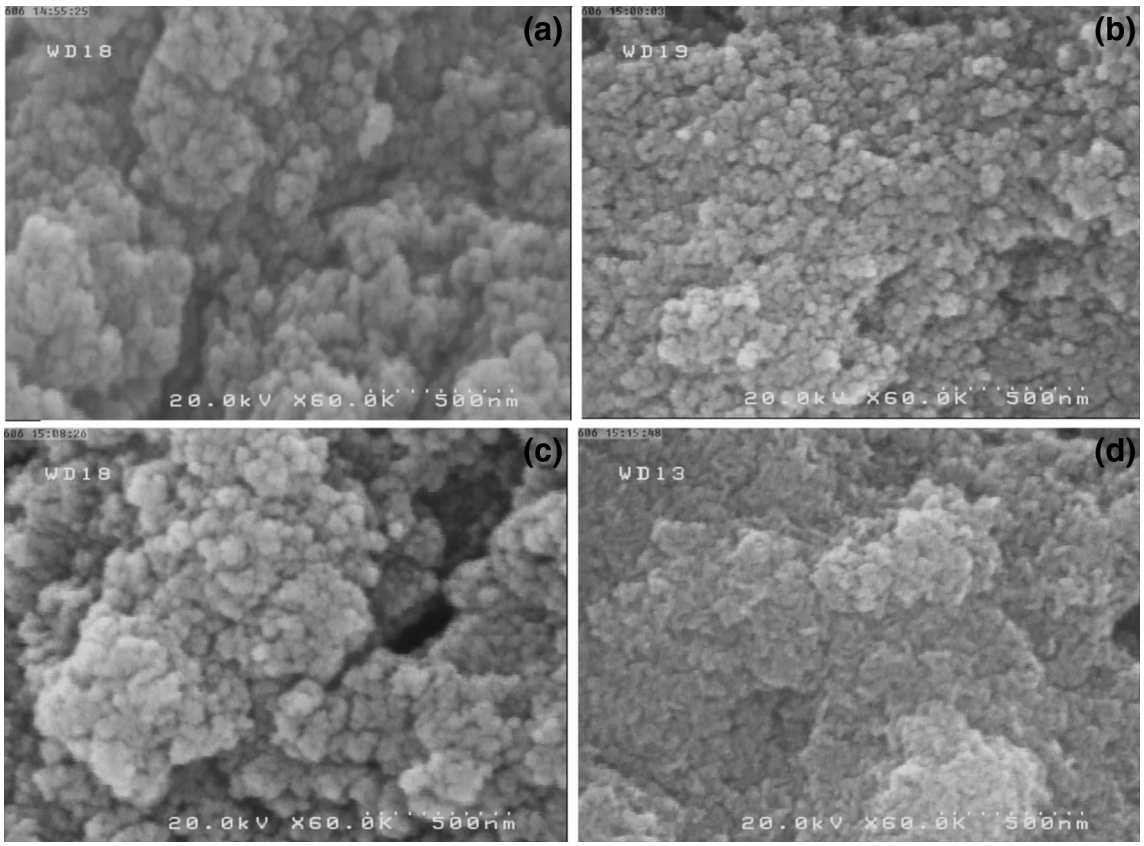

Fig. 1 FESEM images for nickel sulfide nanoparticles precipitated at different conditions of proposed procedure: **a** run 1, **b** run 2, **c** run 5, and **d** run 7

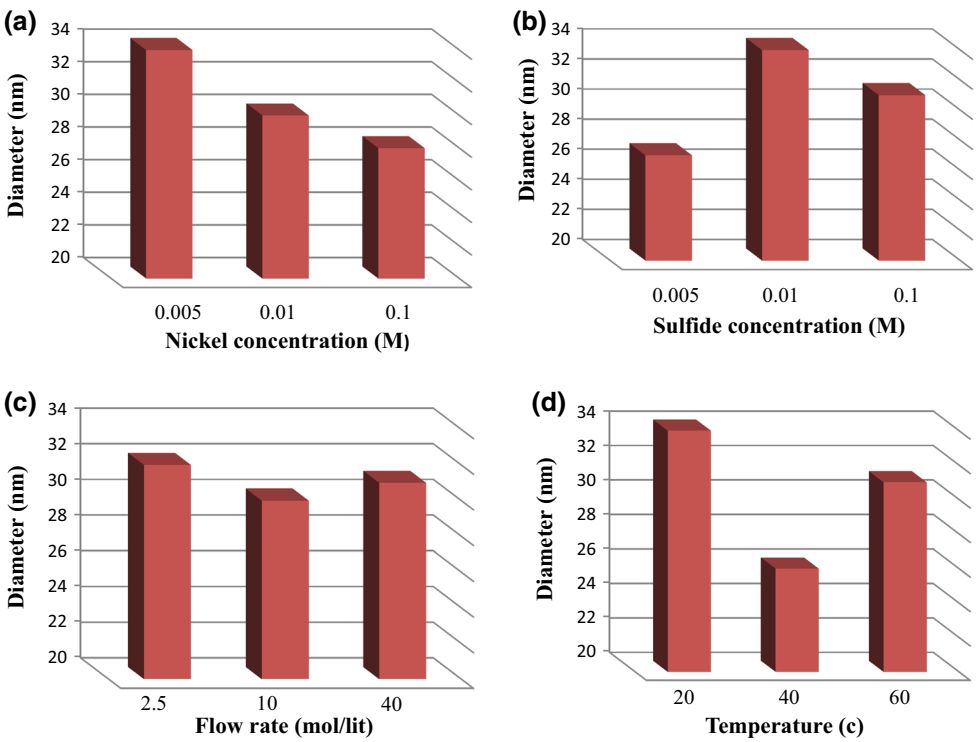

Fig. 2 Average effect of different levels of investigated parameters on the size of nickel sulfide particles

Table 2 Results of ANOVA for synthesis of nickel sulfide nanoparticles by proposed chemical precipitation reaction using OA_9 (3^4) matrix and particle size of synthesized nickel sulfide (nm) as responses

Factor	Code	DOF	S	V	Pooled[a]			
					DOF	S′	F′	P′
Ni^{2+} concentration (mol/L)	C_{Ni}	2	62.89	31.44	2	60	21.77	20.48
S^{2-} concentration (mol/L)	C_S	2	66.89	33.44	2	64	23.15	21.85
Flow rate (mL/min)	F_{Ni}	2	2.89	1.44	–	–	–	–
Temperature (°C)	T_r	2	160.22	80.11	2	157.33	55.46	53.72
Error	E	–	–	–	2	–	–	3.95

[a] The critical value was at 90 % confidence level; pooled error results from pooling insignificant effect

levels of Ni^{2+} concentration, S^{2-} concentration, and temperature, respectively. Thereafter, the value of the confidence interval (CI) corresponds to the size of nickel sulfide nanoparticles at optimum conditions of synthesis procedure is obtained as follows [40, 41]:

$$CI = \pm\sqrt{\frac{F_\alpha(f_1, f_2) \cdot V_e}{n_e}}$$

In this equation, V_e corresponds to the variance of error, $F_\alpha(f_1, f_2)$ is the critical value for F at the level of significance α (90 %), f_1 and f_2 are degree of freedom (DOF), while $f_1 =$ DOF for mean (which always equals 1) and $f_2 =$ DOF for error term. Meanwhile, n_e as the number of effective replications could be obtained as follows:

$$n_e = \frac{Number\ of\ trials}{DOF\ of\ mean\ (always\ 1)\ +\ DOF\ of\ all\ factors\ at\ optimum\ conditions}$$

Calculations showed that the size of nickel sulfide particles at optimum conditions of precipitation procedure will be approximately within 20 ± 3 nm. Consideration of Table 1 confirms that seventh trial in this table is including the proposed optimum conditions of the process (0.1 mol/L as concentration of nickel reagent, 0.005 mol/L concentration of sulfide ion reagent, and 40 °C as the temperature of the reactor). As seen in Fig. 1d, FESEM image for the synthesized nickel sulfide nanoparticles during this experiment (run 7) have an average size about 20 nm which is compatible with the expected range for the size of nickel sulfide nanoparticles at the optimum conditions of precipitation (20 ± 3 nm). Meantime, Fig. 3 shows TEM image of as-synthesized nanoparticles at the optimum conditions (run 7). As seen, the obtained result by SEM is confirmed by TEM image. Thereafter, nickel sulfide nanoparticles obtained at optimum conditions were characterized to confirm their structure, composition, thermal stability and optical behavior by different techniques i.e., XRD, FT-IR, TGA/DSC, and DRS.

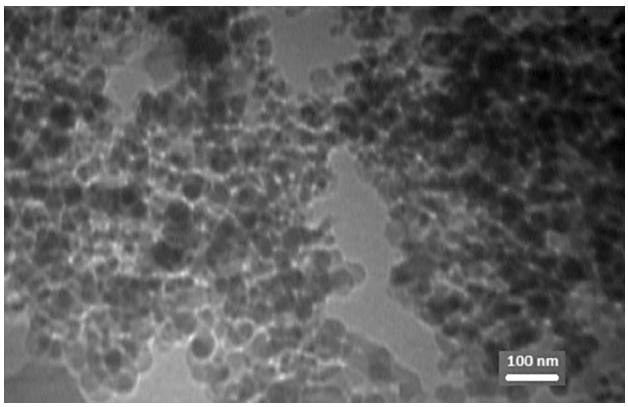

Fig. 3 TEM image of nickel sulfide prepared at optimum conditions

3.2 Characterization of nickel sulfide nanoparticles

The nickel sulfide nanoparticles obtained at optimum conditions of the proposed chemical precipitation process were characterized at first step by X-ray powder diffraction (XRD) to evaluate their structure and composition. XRD pattern of the prepared nickel sulfide nanoparticles is shown in Fig. 4a. As seen, the as-prepared nanoparticles have a low crystallinity. To improve the crystallinity and reduce the presence of impurities, the nanoparticles were dispersed in distillated water, and then transferred to 50 mL Teflon lined stainless steel autoclave [42] and heated to 190 °C for 12 and 24 h in an electrical oven. Then, the resulted particles were rinsed several times and washed with ethanol and were dried at 80 °C for 2 h (Sample h). Figure 4b shows the XRD pattern of this sample. It shows that treatment of the sample at 190 °C for 24 h leads to elimination of impurities from the sample and makes the product more crystalline. The diffraction peaks indexed in this pattern is consistent with the nickel sulfide pattern (a composite of Ni_3S_2 in JCPDS 44-1418 and NiS according to JCPDS 12-0041, diffraction software). Also, the average particle size of the product was estimated by the Scherrer equation [43, 44]:

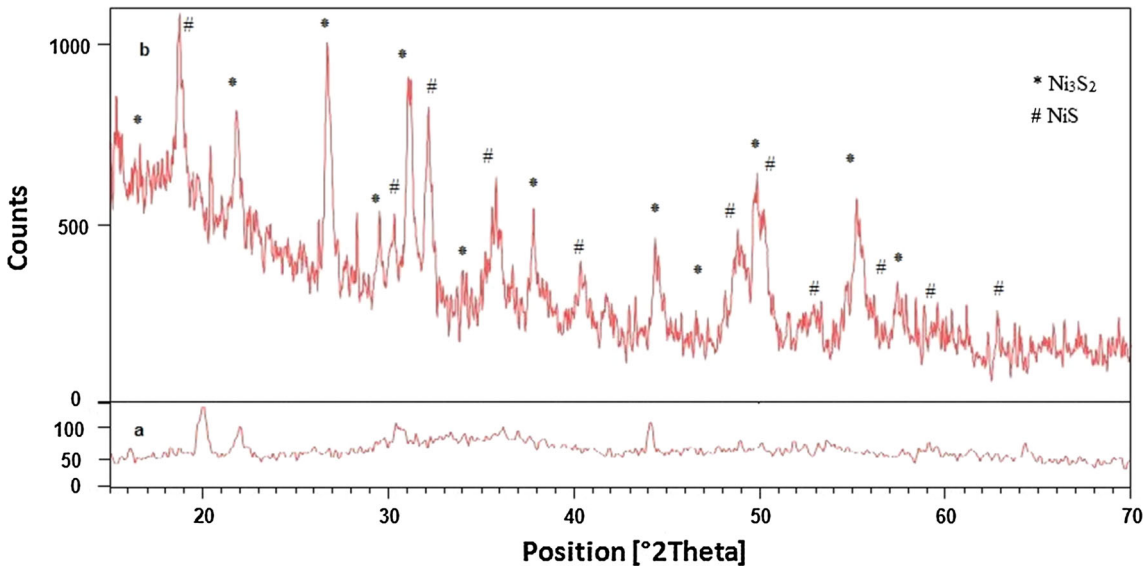

Fig. 4 XRD pattern of nickel sulfide nanoparticles: *a* prepared at optimum conditions of chemical precipitation method; *b* Sample h (after treatment at 190 °C for 24 h)

$$D = \frac{0.9\lambda}{\beta \mathrm{Cos}\theta}$$

where θ is the peak position angle, λ is wavelength of the X-ray radiation and β is the width of appeared diffraction line at its half-maximum intensity. The results show that the average crystalline size of the obtained nickel sulfide particles (Sample h) varies between 20–45 nm.

Figure 5 shows UV–Vis absorption spectrum of as-synthesized NiS nanoparticles dispersed in the distilled water via sonication. The resulted UV absorption peak observed around 218 nm confirms the formation of nano-sized nickel sulfide particles, while their narrow particle size distribution and uniformity of particles is confirmed based on the narrow width of this absorption peak [45].

FT-IR spectroscopy was applied to investigate composition of precipitated nickel sulfide nanoparticles. Figure 6a shows FT-IR spectrum for the nickel sulfide sample prepared at optimum conditions of chemical precipitation which it shows some impurities. Figure 6b shows the FT-IR spectrum of Sample h (the resulted product after applying hydrothermal conditions). The vibrations appeared in the spectrum were in accordance with the previous report on nickel sulfide [42, 43]. However, the observed peaks at 3476 and 1675 cm^{-1} are responsible for the absorption of H_2O in the sample and the formation of hydrated nickel sulfide nanoparticles. The peak position at 652 cm^{-1} is allocated to the Ni–S–Ni bending vibration mode.

Figure 7a shows the UV–Vis diffuse reflectance spectroscopy (DRS) of as-prepared nanoparticles. The diffuse reflectance data was used to measure the optical band gap energy of nickel sulfide nanoparticles. The optical band gap

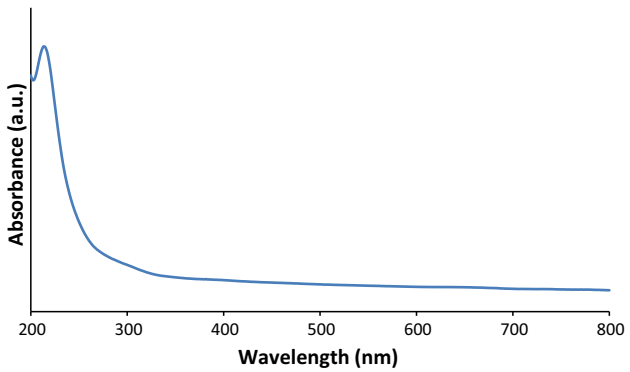

Fig. 5 UV–Vis absorption spectrum of as-synthesized NiS nanoparticles

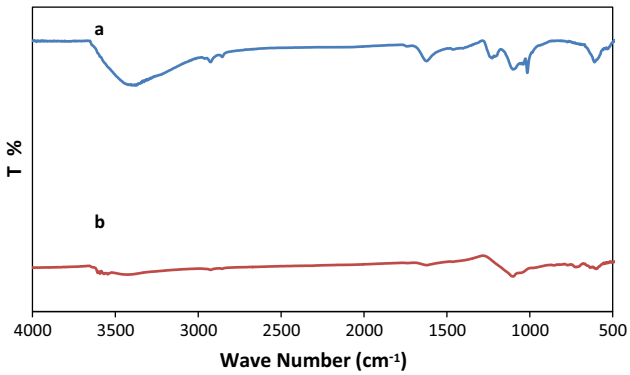

Fig. 6 FT-IR spectrum for nickel sulfide nanoparticles obtained **a** by chemical precipitation, **b** after treatment of as-prepared nanoparticles at 190 °C for 24 h (Sample h)

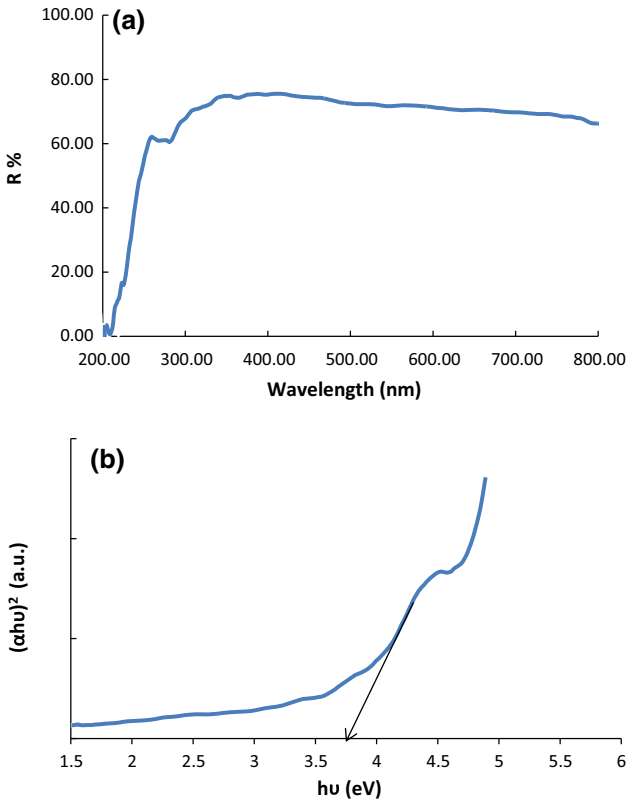

Fig. 7 **a** UV–Vis diffuse reflectance spectroscopy of as-prepared nickel sulfide nanoparticles. **b** Tauc's plot for as-prepared nickel sulfide nanoparticles

energy is defined as the minimum photon energy required exciting an electron from the valence band to conduct band of a semiconductor. The energy dependence of the semiconductors absorption edge is given by Tauc's equation [46]:

$$\alpha \cdot h \cdot \upsilon = A \cdot \left(h \cdot \upsilon - E_g\right)^{\eta}$$

where h, υ, α, E_g, and A are the Planck's constant, frequency of light, absorption coefficient, band gap energy and a proportional constant, respectively. The value of exponent η is respectively 1/2 and 2 for direct and indirect transitions. In this study η is equal to 1/2 for nickel sulfide nanoparticles. Figure 7b shows Tauc's plot for nickel sulfide nanoparticles. As shown the estimated band gap for this sample is approximately 3.75 eV that revealed an absorption edge in about the 330 nm.

The results of characterization studies showed that the properties and behavior of nickel sulfide nanoparticles synthesized via chemical precipitation, in our study, are similar to the nano-particles obtained via other methods [20–24]; while, preparation of nickel sulfide nanoparticles via the proposed method in this study is simple, and cost effective without need to use any template, surfactant, or catalyst.

3.3 Photocatalytic activities

To evaluate the potential of synthesized nickel sulfide nanoparticles in water treatment, their ability to degrade methylene blue (MB) as an organic pollution was investigated. In order to study the photocatalytic degradation kinetic of the MB a pseudo first order kinetic model was used, which is normally used for photocatalytic degradation when the initial concentration of the dye is low. The kinetic model is expressed with the following equation [46–49]:

$$-\frac{dC}{dt} = kC$$

where C, k, t and $-\frac{dC}{dt}$ represent the concentration of MB, reaction rate constant, time of degradation and reaction rate, respectively. Figure 8a gives UV–Vis absorption spectra of the studied solutions, while the plot of C/C_0 (the ratio of MB concentration to the initial concentration) versus time is shown in Fig. 8b. As the results showed after 160 min maximum degradation (about 98.5 %) of MB was achieved. This result suggests that nickel sulfide nanoparticles could be utilized as a hopeful and effective photocatalyst for removal of organic pollutants, i.e., MB from water.

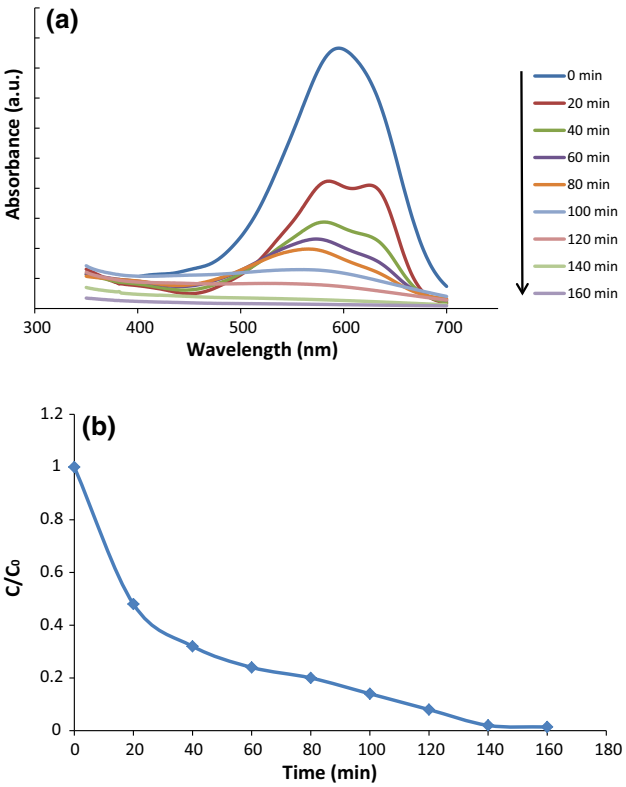

Fig. 8 **a** UV–Vis absorption spectra of MB solution during degradation in the presence of as-synthesized nanoparticles. **b** Photocatalytic performance of as-synthesized nanoparticles

4 Conclusion

Nickel sulfide nanoparticles were successfully prepared via a facile and cost-effective chemical precipitation reaction at optimum conditions without usage any template, surfactant, or catalyst. Produced nickel sulfide samples by the proposed route were composed of the spherical nanoparticles. The composition and structure of the produced nickel sulfide powder at optimum conditions were studied by FESEM, TEM, XRD, FT-IR and DRS analysis. The results of this study clearly confirmed the formation of nickel sulfide nanoparticles. Furthermore, photocatalytic activity of the as-prepared nanoparticles was studied and the results revealed the potential of the synthesized nickel sulfide nanoparticles as a photocatalyst in organic pollutant degradation.

References

1. H.R. Rajabi, M. Farsi, Mater. Sci. Semicond. Process. **31**, 478 (2015)
2. H.R. Rajabi, M. Farsi, J. Mol. Catal. A: Chem. **399**, 53 (2015)
3. S.M. Pourmortazavi, Z. Marashianpour, M. Sadeghpour Karimi, M. Mohammad-Zadeh, J. Mol. Struct. **1099**, 232 (2015)
4. H.R. Rajabi, O. Khani, M. Shamsipur, V. Vatanpour, J. Hazard. Mater. **250–251**, 370 (2013)
5. S.M. Pourmortazavi, S.S. Hajimirsadeghi, M. Rahimi-Nasrabadi, I. Kohsari, Synth. React. Inorg. Met. Org. Chem. **42**, 746 (2012)
6. J. Hu, T.W. Odom, C.M. Lieber, Acc. Chem. Res. **32**, 435 (1999)
7. X. Peng, L. Manna, W.D. Yang, J. Wickham, E. Sher, A. Kadavanich, A.P. Alivisatos, Nature **404**, 59 (2000)
8. J.G. Yu, J.C. Yu, W.K. Ho, L. Wu, X.C. Wang, J. Am. Chem. Soc. **126**, 3422 (2004)
9. Z.W. Pan, Z.R. Dai, Z.L. Wang, Appl. Phys. Lett. **80**, 309 (2002)
10. S. Sun, C.B. Murray, D. Weller, L. Folks, A. Moser, Science **287**, 1989 (2000)
11. S.M. Pourmortazavi, A. Zaree, S. Mirsadeghi, J. Sol-Gel Sci. Technol. **76**, 510 (2015)
12. K. Jacobs, D. Zaziski, E.C. Scher, A.B. Herhold, A.P. Alivisatos, Science **293**, 1803 (2001)
13. C.H. An, Z. Zhang, X. Chen, Y. Liu, Mater. Lett. **60**, 3631 (2006)
14. M. Salavati-Niasari, Gh Banaiean-Monfared, H. Emadi, M. Enhessari, C. R. Chim. **16**, 929 (2013)
15. S.C. Han, H.S. Kim, M.S. Song, J.H. Kim, H.J. Ahn, J.Y. Lee, J. Alloys Compd. **351**, 273 (2003)
16. M. Salavati-Niasari, F. Davar, M. Mazaheri, Mater. Res. Bull. **44**, 2246 (2009)
17. J. Grau, M. Akinc, J. Am. Ceram. Soc. **79**, 1073 (1996)
18. D.W. Bishop, P.S. Thomas, A.S. Ray, Mater. Res. Bull. **33**(9), 1303 (1998)
19. Y.H. Zhang, Q. Wang, Adv. Mater. Res. **366**, 318 (2012)
20. C. Tang, C. Zang, J. Su, D. Zhang, G. Li, Y. Zhang, K. Yu, Appl. Surf. Sci. **257**, 3388 (2011)
21. F. Cao, R.X. Liu, L. Zhou, S.Y. Song, Y.Q. Lei, W.D. Shi, F.Y. Zhao, H.J. Zhang, J. Mater. Chem. **20**, 1078 (2010)
22. L.M. Lang, Z. Xu, Chem. J. Chin. Univ.-Chin. **32**, 584 (2011)
23. M.Y. Liu, N.-N. Shan, C.-H. Guo, C.-M. Lin, Z.-L. Xu, D. Bai, Chin. J. Inorg. Chem. **27**, 1219 (2011)
24. P.F. Yang, B. Song, R. Wu, Y.F. Zheng, Y.F. Sun, J.K. Jian, J. Alloys Compd. **481**, 450 (2009)
25. L. Tian, L.Y. Yep, T.T. Ong, J. Yi, J. Ding, J.J. Vittal, Cryst. Growth Des. **9**, 352 (2009)
26. S.S. Huang, K.D.M. Harris, E. Lopez-Capel, D.A.C. Manning, D. Rickard, Inorg. Chem. **48**, 11486 (2009)
27. S.M. Pourmortazavi, S.S. Hajimirsadeghi, M. Rahimi-Nasrabadi, J. Dispers. Sci. Technol. **33**, 254 (2012)
28. C. Karagiozov, D. Momchilova, Chem. Eng. Process. **44**, 115 (2005)
29. R.K. Roy, *A Primer on the Taguchi Method* (Van Nostrand Reinhold, New York, 1990)
30. G. Taguchi, *Systems of Experimental Design*, vol. 1–2 (Kraus, New York, 1987)
31. S.M. Pourmortazavi, S.S. Hajimirsadeghi, M. Rahimi-Nasrabadi, M.M. Zahedi, Mater. Sci. Semicond. Process. **16**, 131 (2013)
32. P.J. Ross, *Taguchi Techniques for Quality Engineering* (McGraw-Hill, New York, 1988)
33. M. Rahimi-Nasrabadi, A.A. Davoudi Dehaghani, S.M. Pourmortazavi, S.S. Hajimirsadeghi, M.M. Zahedi, CrystEngComm **15**, 4077 (2013)
34. S.G. Hosseini, S.M. Pourmortazavi, M. Fathollahi, Sep. Sci. Technol. **39**, 1953 (2004)
35. M.J. Davidson, G.R.N. Tagore, K. Balasubramanian, Mater. Manuf. Process. **23**, 539 (2008)
36. S.M. Pourmortazavi, M. Taghdiri, N. Samimi, M. Rahimi-Nasrabadi, Mater. Lett. **121**, 5 (2014)
37. V.N. Gaitonde, S.R. Karnik, J.P. Davim, Mater. Manuf. Process. **23**, 377 (2008)
38. S.M. Pourmortazavi, M. Rahimi-Nasrabadi, M. Khalilian-Shalamzari, H.R. Ghaeni, S.S. Hajimirsadeghi, J. Inorg. Organomet. Polym. **24**, 333 (2014)
39. M. Shamsipur, S.M. Pourmortazavi, S.S. Hajimirsadeghi, M. Roushani, Colloid Surf. A **423**, 35 (2013)
40. M. Shamsipur, M. Roushani, S.M. Pourmortazavi, Mater. Res. Bull. **48**, 1275 (2013)
41. S. Ramesh, L. Karunamoorthy, K. Palanikumar, Mater. Manuf. Process. **23**, 174 (2008)
42. M. Salavati-Niasari, F. Davar, H. Emadi, Chalcogenide Lett. **7**, 647 (2010)
43. Y. Fazli, S.M. Pourmortazavi, I. Kohsari, M. Sadeghpur, Mater. Sci. Semicond. Process. **27**, 362–367 (2014)
44. H. Emadi, M. Salavati-Niasari, F. Davar, Polyhedron **31**, 438 (2012)
45. M. Rahimi-Nasrabadi, S.M. Pourmortazavi, M. Khalilian-Shalamzari, J. Mol. Struct. **1083**, 229 (2015)
46. J. Tauc, R. Grigorovici, A. Vancu, Phys. Status Solidi **15**, 627 (1966)
47. CZh Yong, N.D. Zhen, W.L. Kun, Zh Ming, D.D. Dionysios, ACS Appl. Mater. Interfaces **3**, 1528–1537 (2011)
48. V. Vuppala, M.G. Motappa, S.S. Venkata, P.H. Sadashivaiah, Eur. J. Chem. **3**(2), 191–195 (2012)
49. J. Mu, C. Shao, Z. Guo, Z. Zhang, M. Zhang, P. Zhang, B. Chen, Y. Liu, ACS Appl. Mater. Interfaces **3**, 590–596 (2011)